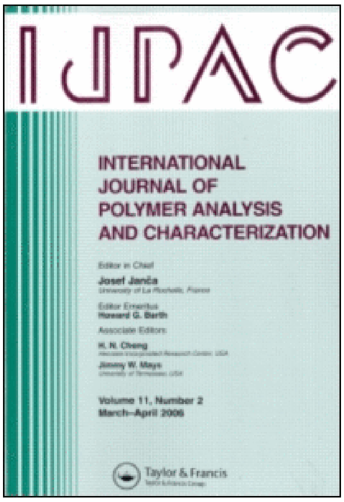

International Journal of Polymer Analysis and Characterization
Publication details, including instructions for authors and subscription information:
http://www.informaworld.com/smpp/title~content=t713646643

Characterization of Hemicellulose B from Corn Fiber by High-Performance Size Exclusion Chromatography with On-Line Molar Mass and Viscometric Detection

Marshall L. Fishman[a]; Landis W. Doner[a]; Hoa K. Chau[a]; Peter D. Hoagland[a]
[a] U. S. Department of Agriculture, Eastern Regional Research Center, Agricultural Research Service, Wyndmoor, PA, USA

To cite this Article Fishman, Marshall L. , Doner, Landis W. , Chau, Hoa K. and Hoagland, Peter D.(2000) 'Characterization of Hemicellulose B from Corn Fiber by High-Performance Size Exclusion Chromatography with On-Line Molar Mass and Viscometric Detection', International Journal of Polymer Analysis and Characterization, 5: 4, 359 — 379

To link to this Article: DOI: 10.1080/10236660008034633

URL: http://dx.doi.org/10.1080/10236660008034633

Int. J. Polym. Anal. Charact.,
2000 Vol. 5, pp. 359–379
Reprints available directly from the publisher
Photocopying permitted by license only

Characterization of Hemicellulose B from Corn Fiber by High-Performance Size Exclusion Chromatography with On-Line Molar Mass and Viscometric Detection*

MARSHALL L. FISHMAN[†], LANDIS W. DONER,
HOA K. CHAU and PETER D. HOAGLAND

U.S. Department of Agriculture, Eastern Regional Research Center, Agricultural Research Service, 600 East Mermaid Lane, Wyndmoor, PA 19038-8598, USA

(Received 3 November 1998; In final form 24 February 1999)

Hemicellulose B (arabinoxylan, corn fiber gum, CFG) was prepared from corn fiber (CF) by alkaline extraction with 2 meq/g of CF using either NaOH, $Ca(OH)_2$ or an equimolar mixture of the two. Prior to CFG extraction, oil was removed from CF by extraction with hexane and starch was removed from CF by treatment with α-amylase. The solutions of alkali-extracted CFG were then bleached with alkaline H_2O_2. The effect of extractant composition on the weight-average molar mass M_w, weight-average intrinsic viscosity $[\eta]_w$, and z-average root-mean-square radius of gyration R_{gz} on CFG was determined. Depending on extractant composition and method of calculation, M_w ranged from $2.7–6.96 \times 10^5$, $[\eta]_w$ from 1.87 to 2.00 dL/g and R_{gz} from about 31 to 50 nm. Substituting $Ca(OH)_2$ for NaOH reduced M_w and R_{gz} but had little or no effect on $[\eta]_w$. Chromatographic analysis in conjunction with molar mass detection revealed that molar mass distributions were bimodal. M_w for the high-molar-mass component ranged from about $8.4–16.1 \times 10^5$, whereas M_w ranged from about $1.1–2.1 \times 10^5$ for the low-molar-mass component. The high-molar-mass component comprised about 15–43% by weight of CFG and was much more compact in shape than the low-molar-mass component.

Keywords: Hemicellulose B; Size exclusion chromatography (SEC);
Multi-angle laser light scattering detector; Viscometric detector; Molar mass;
Intrinsic viscosity

---

*Mention of brand or firm name does not constitute an endorsement by the U.S. Department of Agriculture above others of a similar nature not mentioned.

[†]Corresponding author.

INTRODUCTION

The water-soluble polysaccharide, hemicellulose B, a.k.a. corn fiber gum (CFG), is a potential coproduct from the wet milling of corn. Wet milling of corn is a process for removing corn oil and starch from corn; the residue is corn fiber (CF). Potentially, up to 1.7 million tons/year of CFG could be produced from CF. CF gum has several useful and therefore valuable properties that could be exploited commercially. These properties include being an adhesive, stabilizer, thickener, film former and emulsifier.[1,2] Nevertheless, CFG is not produced commercially and most of the CF produced is used as animal feed. The potentially valuable CFG is not utilized because of technical and cost barriers which are now being overcome.

Hemicelluloses are the major components of corn bran[3] and CF[1,4] and are arabinoxylans. Work performed on CF[4] revealed that up to 40% wt of CF could be obtained as hemicellulose B. Also that the β-$(1 \rightarrow 4)$-D-xylopyranose backbone of hemicellulose B was highly populated with arabinofuranosyl branches. Typically, the sugar composition of hemicellulose B is arabinose 37.7–40.8%, xylose 48.1–49.5%, galactose 5.4–8.4%, glucuronic acid 4.2–4.9%, and glucose 0.8–1.0%.

Recently, we developed novel processes[1,4] for the isolation of CFG in the form of a very white powder. Previously, we have reported[4] the weight-average molar mass M_w of two of the three hemicellulose B fractions that were isolated but were not analyzed in terms of their shape or size (root-mean-square radius of gyration, R_g). Because the functional properties of a polysaccharide are heavily influenced by their global structural properties, we present a more detailed characterization in solution of the hemicellulose B fractions that we have isolated. We also determine and compare M_w and R_{gz} by two methods. One method uses up to 15 scattering angles to determine M_w and R_{gz}, whereas the other method uses the 90° scattering angle in combination with viscometry.

EXPERIMENTAL

Corn Fiber Samples

Fiber samples were provided by American Maize Products Co. (Hammond, IN), Cargill Central Research (Minneapolis, MN), and

CPC Corn Products Division (Summit-Argo, IL). CF was ground to a particle size of 20 mesh using a Wiley mill.

Extraction and Isolation of Hemicellulose B

The extraction and isolation of hemicellulose B from CF is described elsewhere.[1,4] Briefly, starch was removed with a commercial Termamyl α-amylase. CFG was extracted from destarched CF by treating with 2 meq alkali/g fiber. The alkali was either NaOH, $Ca(OH)_2$, or a mixture of the two. The isolated extracts were treated with H_2O_2 at pH 11.5 to whiten the gum, and hemicellulose A was allowed to precipitate by lowering the pH to 4.5. After removal of hemicellulose A, the hemicellulose B was precipitated with 95% ethanol. This last step also serves to separate polysaccharides from extraneous material in the sample.

Preparation of Hemicellulose B for Chromatography

Dried CFG was dialyzed against three changes of HPLC-grade water in a 10,000 MW cut-off dialysis tubing and lyophilized. Dialysis removed a small amount of salt. Forty mg of lyophilized material was dissolved in 20 mL of 50 mM $NaNO_3$, centrifuged at 50,000× *g* for 10 min, allowed to pass through a 0.22-µm sterile Millex-GV filter (Millipore Corp. Bedford, MA) and 100 µL of sample was injected. The mobile phase was 50 mM $NaNO_3$ which was filtered with a 0.2-µm Nucleopore (Costar Corp. Cambridge, MA) membrane filter before degassing.

Chromatography

The chromatography system consisted of a model KT-35 Shodex degasser (JM Science Inc. Grand Island, NY) connected in series to a model 1050 autosampler and pump (Hewlett-Packard Corp.), in-line 0.1-µm Durapore vv membrane filter housed in a high-pressure holder (Millipore Corp. Bedford, MA), 15′ stainless-steel warming coil, i.d. 0.04″, two (10 × 3.2-mm i.d.) Synchropak cartridge guard columns (one pre- and one post-column set (Micra Scientific, Inc. Northbrook, IL), and three chromatography columns. The serially placed chromatography columns were, two PL- Aquagel OH-60 and one OH-40 (Polymer Labs. Amherst, MA). The exclusion limits for these columns, as specified by the manufacturer for polyethylene glycol, were 2×10^7 and 1×10^5 g/mol, respectively. Each column was 7.5-mm i.d. × 300-mm length. The nominal flow rate was 0.7 mL/min. Columns were thermoregulated at 45°C by immersing them in a water bath. A model Dawn F multi-angle laser light scattering detector (MALLS) fitted with a helium–neon laser ($\lambda = 632.8$ nm) and a K-5 flow cell (Wyatt Technology, Santa Barbara, CA), a model 100 differential pressure viscometer detector (DP) (Viscotek Corp. Houston, TX) and a model ERC-7510 differential refractive index monitor (DRI) (ERMA Optical Works, LTD. Tokyo, Japan) were employed.

The electronic outputs from the MALLS at 90° scattering angle, DRI and DP detectors were sent to a Viscotek model DM 400 data manager which, in turn, was interfaced to a 486 computer containing Viscotek Trisec 3.0 GPC software. Simultaneously, the electronic outputs from the MALLS at 15 light scattering angles and the DRI were sent to an A/D board housed in the MALLS which, in turn, was interfaced to a second 486 PC loaded with ASTRA™ (v. 2.11) and ASTRA™ (v. 4.2) software (Wyatt Technology). The data were collected with the ASTRA™ (v. 2.11) software and processed with ASTRA™ (v. 4.2) software.

The DRI response factor was measured by injecting a series of known NaCl concentrations directly into the detector cell with a syringe. This response factor was obtained from the slope of the linear plot between NaCl concentration and RI response. The factor to correct the Rayleigh ratio at 90° (R_{90}) for instrument geometry was obtained by measuring the scattering intensity of toluene at 90° and tested with pullulan standards.[5] The responses to scattered light intensity of the photodiodes arrayed around the scattering cell at angles other than 90° were normalized to the diode at 90° with a P-50 pullulan standard M_w, 48,000. The scattering angles in degrees available for intensity measurements were 22.26, 29.11, 36.46, 44.72, 54.19, 65.02, 77.11, 90.00, 102.89, 114.98, 125.81, 135.28, 143.54, 150.89, and 157.74.

As suggested in Ref. [6], molar masses and radii were extracted from data fit to Debye equations. Data were found to be best fitted by linear least squares to a first-order Debye equation. There was no *ad hoc* deletion of scattering angles in fitting the Debye equations but closeness of line fit to the reduced excess light scattering at a particular angle was weighted. The weighting factor was based on the standard deviation of the scattering at each angle as compared to the average standard deviation of all detectors fitted. The standard deviation of the scattering intensity at the four lowest scattering angles was greatest. Generally, for these angles, the standard deviation increased with decreasing scattering angle. The practical effect of this method was that in some cases the scattering intensity of light from the lower scattering angles fell far from the fitted line. Nevertheless, the line was well fitted to the other eleven angles.

The viscometer was checked with pullulan standards to ensure that intrinsic viscosities were measured accurately. The concentration of hemicellulose B was obtained from the area of its DRI chromatogram. This concentration was calculated using ASTRA software by inputting the concentration dependence of the refractive index (d*n*/d*c*). A d*n*/d*c* value of 0.135 mL/g at 670 nm was determined for hemicellulose B in 50 mM $NaNO_3$, described previously.[7]

RESULTS AND DISCUSSION

Based on weight of sample prior to injection, average recovery from chromatography was greater than 99%. The lowest value was 88%, whereas the highest value was 106%. In Figure 1 are typical superimposed chromatograms of the scattering intensity at 90° (left), the DP (middle) and the DRI (right) for hemicellulose B extracted with NaOH. In Figures 2 and 3, are superimposed chromatograms of the scattering intensity at 90° (left), and the DRI (right) for the same data that was used to obtain the comparable chromatograms in Figure 1. Also in those figures are Debye plots at or near the two relative maxima in the chromatograms. The chromatograms in Figure 1 were generated by the Trisec software, whereas the chromatograms in Figures 2 and 3 were generated by the Astra software. Employing the Trisec software, it is possible to calculate molar masses, intrinsic viscosities and radii of gyration from the data generated by the chromatograms

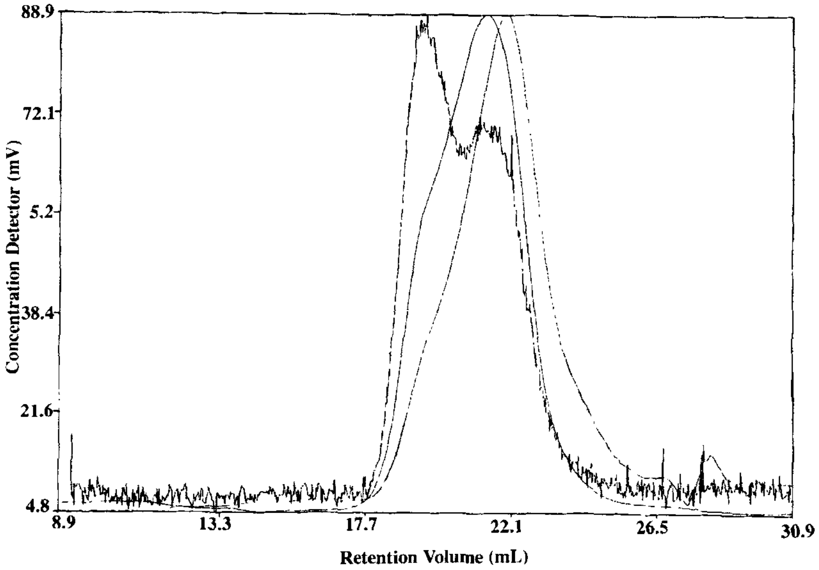

FIGURE 1 Chromatograms for hemicellulose B extracted with NaOH, generated by Trisec software, scattering intensity at 90° (left), the DP (center) and the DRI (right).

in Figure 1, that is the LS/Viscometry method.[8] The Trisec software calculates M_w and R_{gz} as follows:[8]

For dilute solutions, the excess scattering R_θ due to polymer dissolved at concentration c is related to its M_w by

$$Kc/R_\theta = 1/(M_w P(\theta)). \tag{1}$$

Here, K is a constant related to the optical properties of the dissolved polymer given by

$$K = (2\pi^2 n_0^2/\lambda_0^4 N_A)[dn/dc]^2, \tag{2}$$

where, N_A is Avagadro's number, n_0 the refractive index of the solvent, dn/dc the change in refractive index of the solution with concentration of the dissolved polymer, and λ_0 the wavelength of the incident light in vacuum. $P(\theta)$ is the particle scattering function which describes the angular dependence of the excess scattered light radiating from the dissolved polymer. Initially, M_w is estimated (M_{est}) from Equation (1) by assuming that $P(90°) = 1$ and measuring $R_{90°}$. Then a new value of

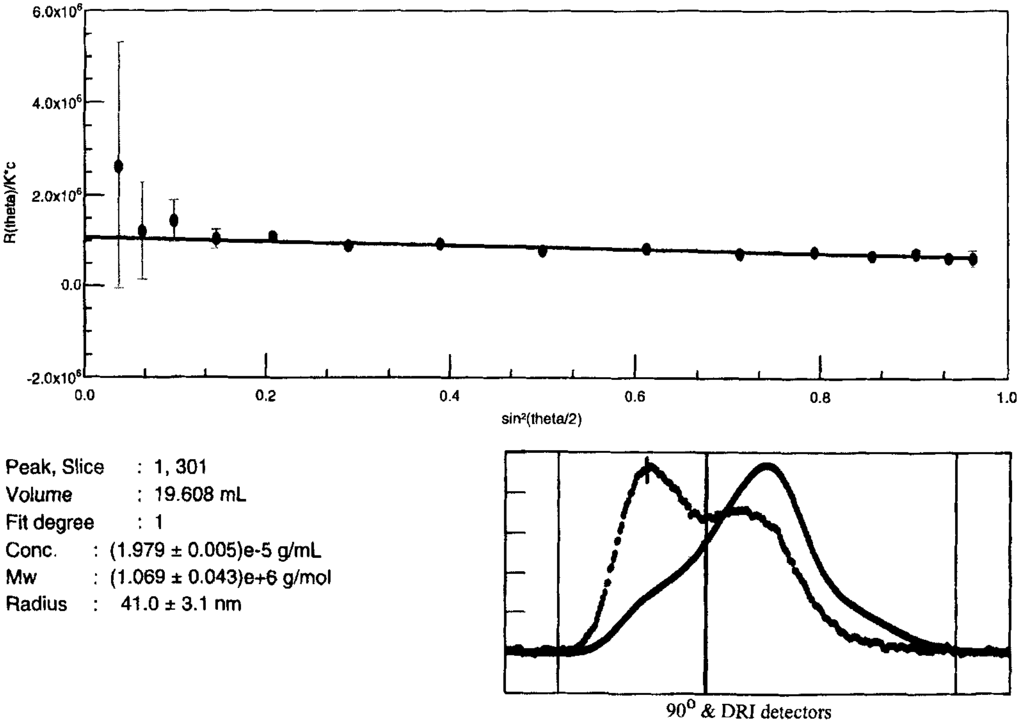

Peak, Slice : 1, 301
Volume : 19.608 mL
Fit degree : 1
Conc. : (1.979 ± 0.005)e-5 g/mL
Mw : (1.069 ± 0.043)e+6 g/mol
Radius : 41.0 ± 3.1 nm

FIGURE 2 Chromatograms for hemicellulose B extracted with NaOH, generated by Astra software, scattering intensity at 90° (left), and DRI (right). Data for peak slice from fraction 1. Vertical lines at ends indicate limits of integration for entire sample. Vertical line in center indicates end of fraction 1 and beginning of fraction 2.

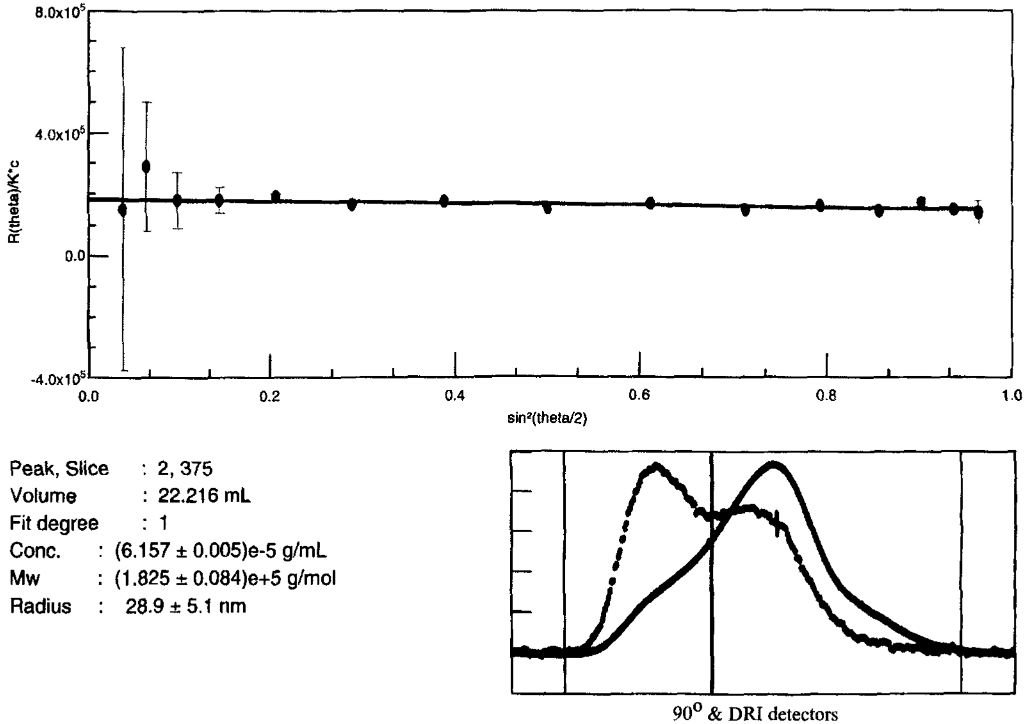

Peak, Slice : 2, 375
Volume : 22.216 mL
Fit degree : 1
Conc. : (6.157 ± 0.005)e-5 g/mL
Mw : (1.825 ± 0.084)e+5 g/mol
Radius : 28.9 ± 5.1 nm

FIGURE 3 Chromatograms for hemicellulose B extracted with NaOH, generated by Astra software, scattering intensity at 90° (left), and the DRI (right). Data for peak slice from fraction 2. Vertical lines at ends indicate limits of integration for entire sample. Vertical line in center indicates end of fraction 1 and beginning of fraction 2.

$P(90°)$ is estimated $P(90°)_{\text{est}}(\text{new})$ from

$$P(90°)_{\text{est}} = 2\left[\frac{\mathrm{e}^{-x}(1-x)}{x^2}\right], \tag{3}$$

where x is given by

$$x = (4\pi n_0/\lambda_0)R_{\text{g}}. \tag{4}$$

Here, R_{g} is estimated from Equation (5), the Pititsyn–Eisner modification of the Flory–Fox equation

$$R_{\text{g,est}} = \left(\frac{1}{6}\right)^{1/2}\left([\eta]\left(\frac{M}{F}\right)\right)^{1/3}, \tag{5}$$

where $[\eta]$ is the intrinsic viscosity IV, and F is obtained from

$$F = 2.86 \times 10^{21}(1 - 2.63e + 2.86e^2)$$

and,

$$e = \frac{(2a-1)}{3}. \tag{6}$$

Here a is the exponent of the Mark–Houwink equation

$$[\eta] = K'M^{\text{a}}. \tag{7}$$

A new value of M_{est}, $M_{\text{est}}(\text{new})$ is calculated from

$$M_{\text{est}}(\text{new}) = \frac{M_{\text{est}}}{P(90°)_{\text{est}}}. \tag{8}$$

Then, $M_{\text{est}}(\text{new})$ is substituted into Equation (5) to obtain $R_{\text{g,est}}(\text{new})$. $R_{\text{g,est}}(\text{new})$ is substituted into Equation (4) to obtain $x(\text{new})$ which in turn is substituted into Equation (3) to obtain $P(90°)_{\text{est}}(\text{new})$. This iteration is repeated until $R_{\text{g,est}}$ is unchanged.

Equation (3) was developed for linear polymers which assume the shape of a random coil when in solution. Comparable equations have been developed for polymers that behave like rigid rods or hard spheres in solution. The software allows one to choose between the three models when processing this data.

The Flory–Fox equation is similar to Equation (5) in that it relates R_g to IV and M. It is derived for a linear, random-coil polymer, dissolved in an ideal solvent.[9] Under these conditions, a random-coil polymer with radius R_g, would have an IV proportional to a sphere with an equivalent volume. The proportionality constant, Φ, is independent of the characteristics of any particular chain and was determined from measurements on a large number of solvent–polymer pairs dissolved in ideal solvents. Furthermore, it was expected that the Flory–Fox equation would hold for many nonlinear polymers as well.[9] The Ptitsyn–Eisner modification of the Flory–Fox equation was developed for polymers dissolved in nonideal solvents by using the Mark–Houwink exponent, a, to experimentally correct for perturbations of the polymer chain away from ideality. Thus the basic concept of the triple detector approach is to calculate R_g from Equation (5). The viscosity and the Mark–Houwink exponent of the fractionated polymer is measured with an on-line differential-pressure viscometer, and the molar mass of the fractionated polymer by light scattering at 90°.

The second approach of measuring R_g and M_w is from the Astra software using scattering intensities at fifteen angles (MALLS), as shown in Figures 2 and 3.[10]

Table I contains data obtained from both the MALLS and the LS/Viscometry methods for various NaOH : Ca(OH)$_2$ ratios in the extractant, with or without alkaline H_2O_2 treatment of the hemicellulose. Data from both methods for the alkaline H_2O_2 generated hemicellulose B, showed a decrease in M_w with increasing ratios of

TABLE I Molecular properties of hemicellulose B

NaOH: Ca(OH)$_2$^{c}	*MALLS*^{a}			*LS/Viscometry*^{b}			
	H_2O_2	$M_w \times 10^{-5}$	R_{gz} (nm)	$M_w \times 10^{-5}$	R_{gz} (nm)	$[\eta]_w$ (dL/g)	a^d
1 : 0	no	3.40(0.09)^e	36(2)	3.61(0.02)	33.5(0.1)	1.98(0.01)	0.66
1 : 0	yes	3.94(0.04)	37(2)	3.87(0.3)	33.7(1.0)	1.92(0.05)	0.84
1 : 1	yes	3.03(0.10)	31(2)	3.40(0.09)	32.7(0.5)	1.94(0.02)	0.67
0 : 1	yes	2.78(0.05)	34(1)	2.97(0.02)	30.8(0.4)	1.89(0.01)	0.73
0 : 1^f	no	3.64(0.07)	34(2)	3.59(0.06)	31.2(0.5)	2.00(0.04)	0.70
1 : 0^g	no	6.96(0.04)	36(1)	8.34(0.02)	42.3(0.1)	1.87(0.2)	0.36

[a]Determined by multi-angle laser light scattering. [b]Determined by combination of light scattering at 90° and viscometry. [c]Ratio of NaOH to Ca(OH)$_2$ in milliequivalents. [d]Mark–Houwink exponent. [e]Standard deviation of triplicate analysis. [f]First step in sequential extraction. [g]Second step in sequential extraction.

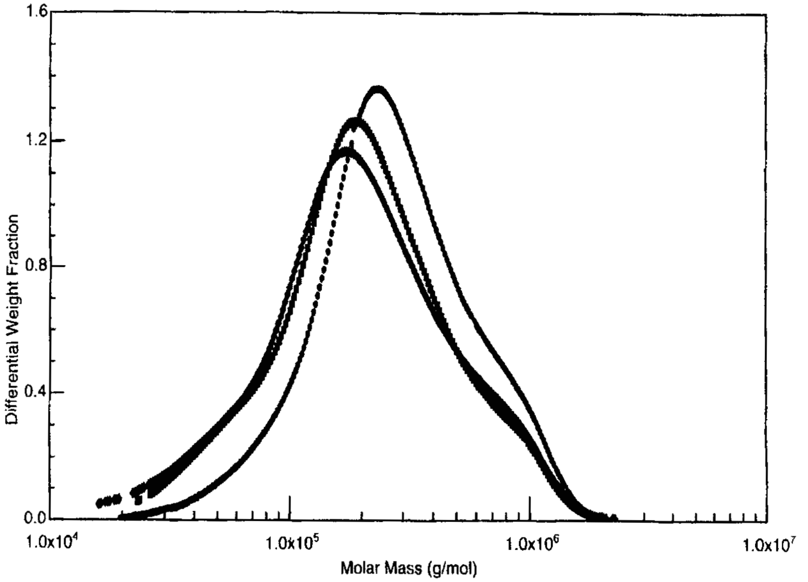

FIGURE 4 Differential molar mass curves. All samples were treated with alkaline H_2O_2, extracted with NaOH (right), extracted with a 1 : 1 milliequivalent mixture of NaOH and $Ca(OH)_2$ (center), extracted with $Ca(OH)_2$ (left).

$Ca(OH)_2$ in the extractant as shown by the superimposed differential molar mass, curves in Figure 4. Figure 5 contains calibration curves of molar mass (M) against volume superimposed upon differential refractive index curves arising from hemicellulose B extracted by three NaOH : $Ca(OH)_2$ ratios and treated with H_2O_2. If column bandspreading for each sample is identical and changing extraction composition does not alter the conformation of the extracted hemicellulose B, amount of overlap between molar mass calibration curves is indicative of the reproducibility of measurements along the breadth of the distribution. Based on that criteria, molar mass measurements are very reproducible between elution volumes of 18.3 and 25 mL for hemicellulose B extracted with ratios of NaOH : $Ca(OH)_2$ of 1 : 1 and 0 : 1. When the comparison includes hemicellulose B extracted with only NaOH as well, the range of complete overlap between polysaccharides from the three extractions is in the range of elution volumes between 18.3 and 22.7 mL. The rising molar mass with elution volume beyond 22.7 mL is caused by light scattering signals with poor signal to noise

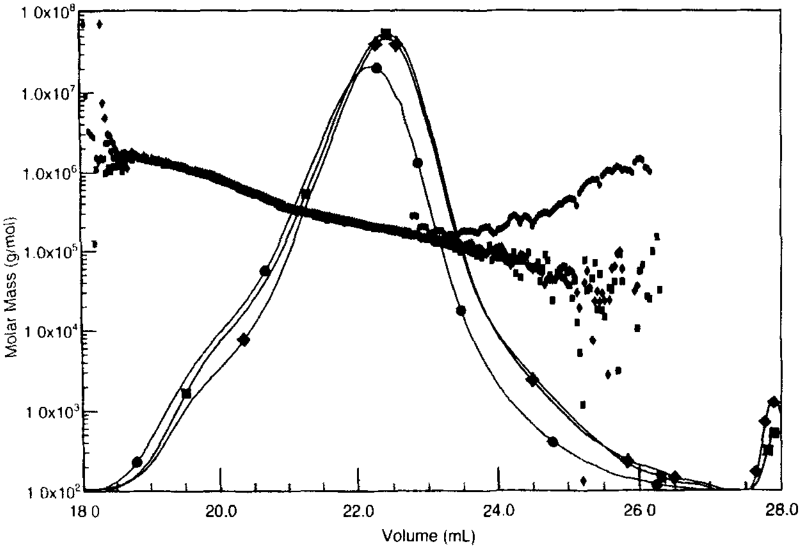

FIGURE 5 Molar mass against volume curves superimposed upon differential refractive index curves for hemicellulose B extracted with three ratios of NaOH : $Ca(OH)_2$ and treated with H_2O_2; (left, ●), NaOH : $Ca(OH)_2$ ratio 1 : 0; (center, ■), NaOH : $Ca(OH)_2$ ratio 1 : 1; (right, ◆), NaOH : $Ca(OH)_2$ ratio 0 : 1.

due to insufficient polysaccharide in the low molar mass tail of the distribution.

To test the hypothesis further that higher molar masses were obtained with NaOH than with $Ca(OH)_2$, CF was extracted sequentially. First CF was extracted with $Ca(OH)_2$ and hemicellulose B was removed. The residue was then extracted with NaOH. This experiment also confirmed that higher molar masses were obtained by the NaOH extraction than by the $Ca(OH)_2$ extraction. We also observed that M_w values were significantly higher for the sequentially extracted samples than for singly extracted CF (e.g., 6.96 and 3.64×10^5 against 3.94 and 2.78×10^5). In the case of the sample sequentially extracted with NaOH, the percentage of high-molar-mass hemicellulose B increased considerably over that in the singly extracted sample as shown by the differential refractive index curve in Figure 6. These differences in M_w may be due to sample heterogeneity and/or CF matrix left more accessible to NaOH extraction, due to prior extraction with $Ca(OH)_2$.

Discrepancies in M_w between the LS/Viscometry method and the MALLS method ranged from about 1.3% to 20%. Four of the six

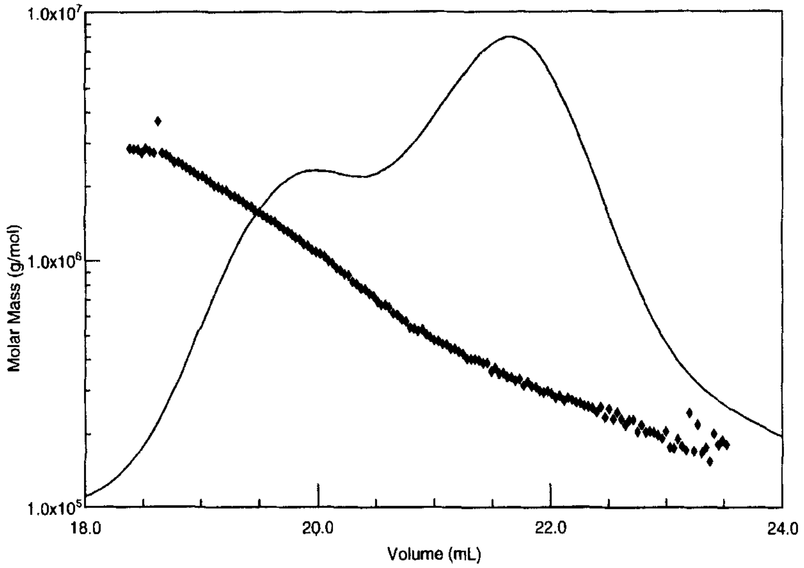

FIGURE 6 Molar mass against volume curve superimposed upon differential refractive index curve for hemicellulose B extracted with NaOH after first extracting with $Ca(OH)_2$.

measurements of M_w were higher by the LS/Viscometry method than by the MALLS method. From the data in Table I, it appears that R_{gz} and $[\eta]_w$ also decrease with increasing $Ca(OH)_2$ ratio as one would expect. Nevertheless, changes in these quantities with $Ca(OH)_2$ ratio are sufficiently small that the trend is only apparent when comparing sample extracted with $Ca(OH)_2$ or NaOH alone.

Recently, Saulnier and coworkers[11] found M_w values of 2.7×10^5 and 3.7×10^5 for hemicellulose from maize bran extracted sequentially with 0.5 M NaOH and 1.5 M KOH, respectively. M_w values are comparable to those in Table I for the singly extracted CF. The intrinsic viscosities for these same two fractions were 1.59 and 1.81 dL/g, respectively.[11] The $[\eta]_w$ values in Table I are slightly higher, in that they range between 1.87 and 2.00 dL/g. It should be mentioned that the pH was found to be different in the extraction soup for each base composition. It ranged from 9.8 in the $Ca(OH)_2$ extraction to *11.1 in* the NaOH extraction (see Ref. [4]). In that paper, yields correlated with pH and in the present study we have shown that the NaOH extracted hemicellulose B had a higher M_w. Nevertheless, results found in this work are consistent with those found by Saulnier and coworkers.[11]

The bimodal nature of the hemicellulose B distribution is clearly delineated by the light scattering chromatograms in Figures 2 and 3. Furthermore, the superimposed Mark–Houwink plots shown in Figure 7, (differential molar mass curves appear in Figure 4), show the bimodal nature of the hemicellulose B distribution as well. The overall Mark–Houwink exponents for all the samples measured are given in Table I. The Trisec software determines these exponents by drawing the best linear least squares first order line through data

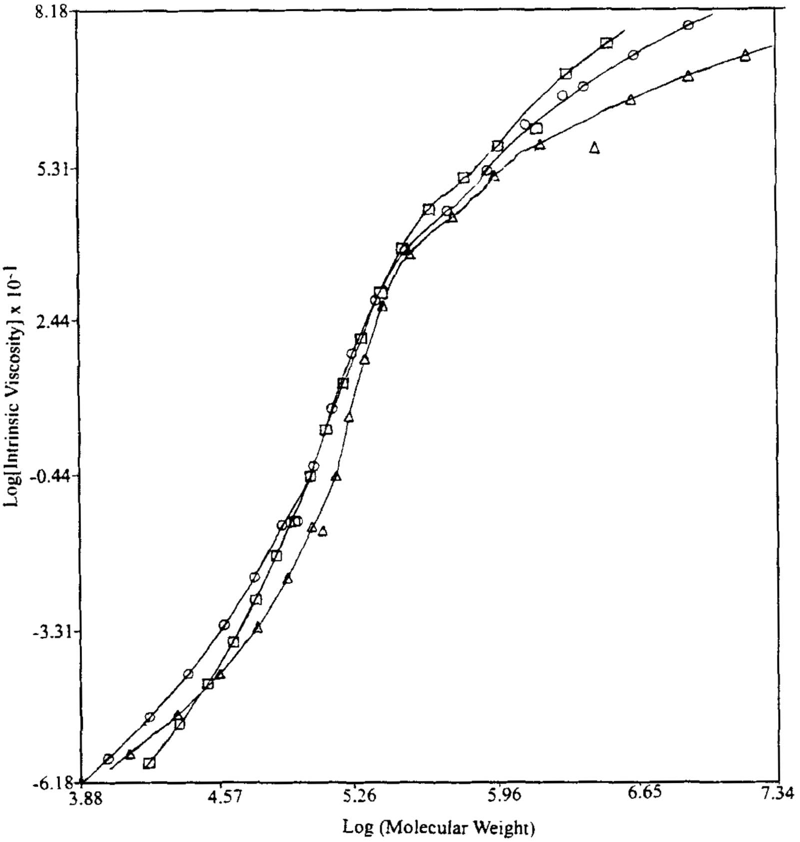

FIGURE 7 Mark–Houwink plots for hemicellulose B extracted with various ratios of NaOH : $Ca(OH)_2$ and treated with H_2O_2; (○), NaOH : $Ca(OH)_2$ ratio 1 : 0; (□), NaOH : $Ca(OH)_2$ ratio 1 : 1; (△), NaOH : $Ca(OH)_2$ ratio 0 : 1.

such as found in Figure 7. Nevertheless, it is clear from the curvilinear nature of these lines that a straight line could not adequately represent the slope of these plots. Therefore, we integrated the chromatograms by parts using elution volumes coincident with the minimum in the 90° light scattering curve to separate the distributions. In this way we were able to calculate the average molecular parameters for molecules in each fraction of the bimodal distribution. The results of these calculations are given in Table II. In fraction 1, LS/Viscometry gave M_w and R_{gz} values which were higher than those given by the MALLS method. In the case of fraction 2, R_{gz} was lower by the LS/Viscometry method than by the MALLS method. Generally, the M_w for fraction 1 was about four or more times greater than fraction 2. Depending on whether the MALLS values of R_{gz} are used or whether the LS/Viscometry values are used, fraction 1 is about 1.3–2.1 times greater in radius than fraction 2. In the column labeled "b" are the power law exponents in the equation relating R_{gz} to M_w, whereas in the column labeled "a" are the Mark–Houwink exponents in the equation relating $[\eta]$ to M.

Figure 8 is a plot of R_g against M whereas Figure 7 contains plots of $[\eta]$ against M. The low values of these exponents indicate an extremely compact structure. For fraction 2, the Mark–Houwink exponents range from 0.71 to 1.41 indicating a much less compact structure. Figure 9 contains calibration curves of root-mean-square radii (R_g) against volume superimposed upon differential refractive index curves arising from hemicellulose B extracted by three NaOH : $Ca(OH)_2$ ratios and treated with H_2O_2. In this case, if column bandspreading for each sample is identical, the amount of overlap between calibration curves is indicative of the reproducibility of radii measurements along the breadth of the distribution. Based on the relatively small discrepancy between calibration curves, radii measurements are reasonably reproducible between elution volumes of 18 and 22.5 mL. That range includes all of fraction 1 and most of fraction 2. Insufficient signal to noise for the angular dependence of the light scattering signal for elution volumes beyond 22.5 mL is responsible for the large scatter in radii values in this fraction of the size distribution. Since this fraction is in the low end of the size distribution, the z-average radius is relatively unaffected by not including it in the calculation.

Fine structure analysis by several groups[11–13] indicates that hemicellulose is highly branched. Possibly, the larger Mark–Houwink

TABLE II Molecular properties of hemicellulose B in bimodal fractions

$NaOH:Ca(OH)_2$[c]	F[d]	*MALLS*[a]				*LS/Viscometry*[b]				
		wt%	$M_w \times 10^{-5}$	R_{gz} (nm)	b[e]	wt%	$M_w \times 10^{-5}$	R_{gz} (nm)	$[\eta]_w$ (dL/g)	a[f]
1:0[g]	1	22.3(0.2)[h]	8.1(0.3)	41(2)	0.21	19.6(0.6)	10.0(0.2)	53(1)	3.5(0.1)	0.27
1:0	1	22.1(1)	7.8(0.1)	39(2)	0.24	19.8(2)	10.1(0.9)	50(2)	3.4(0.2)	0.27
1:1	1	18.4(2)	7.6(0.6)	38(4)	0.26	17.4(2)	9.5(0.7)	50(2)	3.5(0.1)	0.29
0:1	1	18.0(0.6)	7.1(0.6)	39(1)	0.21	16.7(0.4)	8.6(0.5)	49(3)	3.6(0.2)	0.28
0:1[g,i]	1	15.3(0.4)	9.9(0.3)	38(1)	0.19	14.5(0.3)	12.5(0.2)	50(1)	3.1(0.1)	0.26
1:0[g,j]	1	43.1(0.8)	12.8(0.2)	38(1)	0.21	40.7(2)	17.1(0.7)	55(1)	2.5(0.1)	0.20
1:0[g]	2	78.7(0.6)	2.1(0.1)	31(2)	—	80.9(0.1)	2.0(0.1)	24(1)	1.6(0.1)	0.97
1:0	2	73.5(3)	2.7(0.3)	39(2)	—	79.5(2)	2.0(0.1)	24(1)	1.6(0.1)	1.41
1:1	2	80.5(3)	1.8(0.1)	25(6)	—	82.4(0.9)	1.9(0.1)	23(1)	1.6(0.1)	0.96
0:1	2	80.9(2)	1.8(0.1)	30(3)	—	83.9(1)	1.5(0.1)	23(3)	1.5(0.1)	0.97
0:1[g,i]	2	84.8(0.9)	2.4(0.1)	30(3)	—	86.0(0.6)	2.4(0.1)	24(1)	1.4(0.1)	0.83
1:0[g,j]	2	60.3(2)	3.0(0.1)	29(2)	—	56.0(3)	1.4(0.1)	25(1)	1.4(0.1)	0.71

[a] Determination by multi-angle laser light scattering. [b] Determination by combination of light scattering 90° and viscometry. [c] Ratio of NaOH to $Ca(OH)_2$ in milliequivalents. [d] Fraction. [e] Power law constant in equation relating R_{gz} to M_w. [f] Mark–Houwink exponent. [g] No H_2O_2 treatment. [h] Standard deviation of triplicate analysis. [i] First step in sequential extraction. [j] Second step in sequential extraction.

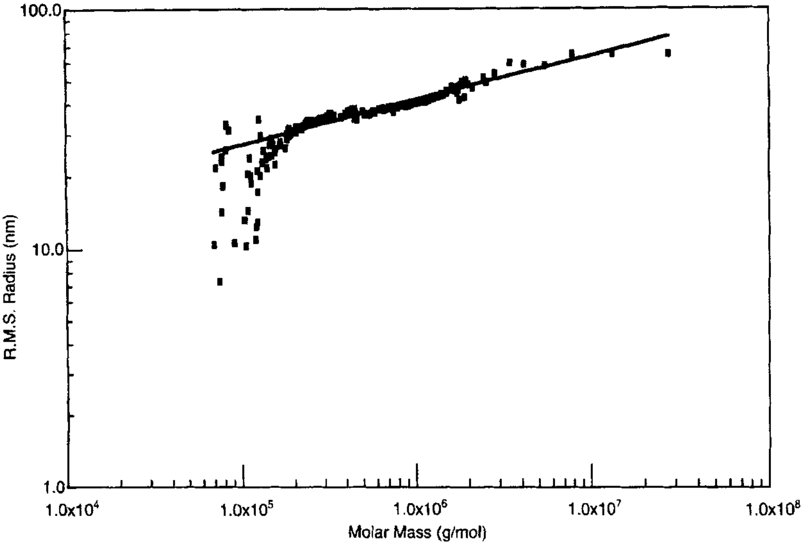

FIGURE 8 Plot of root-mean-square radius (R_g) against molar mass for hemicellulose B extracted with NaOH.

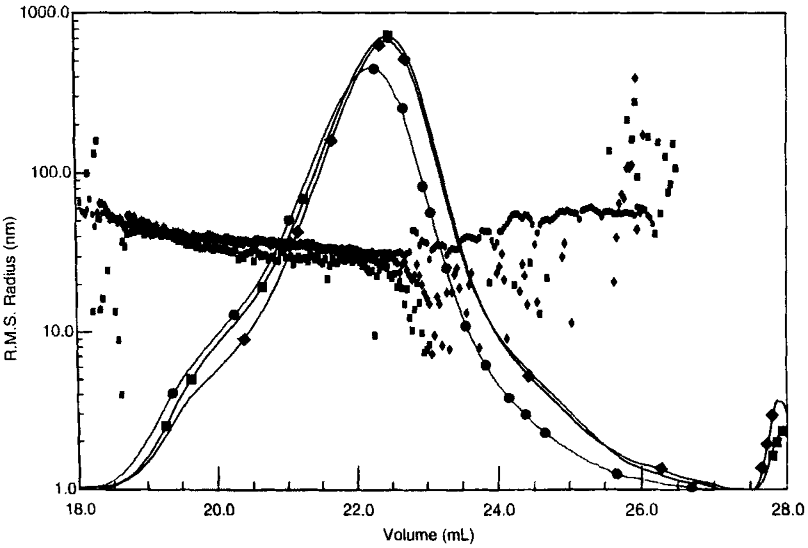

FIGURE 9 Root-mean-square radius (R_g) against volume curves superimposed upon differential refractive index curves for hemicellulose B extracted with various ratios of NaOH : $Ca(OH)_2$ and treated with H_2O_2; (left, ●), NaOH : $Ca(OH)_2$ ratio 1 : 0; (center, ■), NaOH : $Ca(OH)_2$ ratio 1 : 1; (right, ◆), NaOH : $Ca(OH)_2$ ratio 0 : 1.

exponents for fraction 1 as compared to fraction 2 indicates a higher degree of branching for fraction 1 hemicellulose as compared to fraction 2. If this were the case, then the situation could be somewhat similar to starch, which is comprised of two closely related polysaccharides, namely highly branched amylopectin and more linear amylose.[14] In that case, it was found that the M_w of amylopectin in common starch was about 170 times greater than the M_w of amylose, whereas the R_{gz} of amylopectin was only about twice as large as the R_{gz} of amylose.[5] It is interesting to note that sequentially extracted CF sample gave lower Mark–Houwink exponents and IV values and higher M_w values than comparable singly extracted samples. Thus it was indicated that hemicellulose B molecules from the sequential extraction tended to be somewhat more compact than comparable molecules from the single extraction.

As indicated by Equations (3)–(8), an incorrect value of a will produce an incorrect value of R_{gz}, which in turn will lead to incorrect values of $P(90°)$ and M_w. Comparison of a values in Table I with those in Table II reveals that the global values of a found in Table I fall somewhere between the values of a for the individual fractions found in Table II. Because the composition of a distribution that is polydisperse in molar mass and/or size profoundly affects the respective global averages, the effect of bimodality on the global values was investigated. This was accomplished by averaging the sum of the fraction averages according to Equations (9)–(11).

$$(R_g^2)_z^{1/2} = \left\{ \frac{\sum w_i M_{wi} (R_{gz}^2)_i}{\sum w_i M_{wi}} \right\}^{1/2}, \tag{9}$$

$$M_n = \frac{1}{\sum (w_i / M_{ni})}, \tag{10}$$

$$M_w = \sum w_i M_{wi}. \tag{11}$$

Here w_i is the weight fraction of the ith fraction, M_n the number-average molar mass and $(R_g^2)_z^{1/2}$ is the same as R_{gz}. The results of these calculations are in Table III. Also included for purposes of comparison are values from MALLS. Comparisons of LS/Viscometry values before (see Table I) and after (see Table III) correction reveal that corrected M_w values decreased whereas corrected R_{gz} values increased.

TABLE III Corrected molecular properties of hemicellulose B from LS/Viscometry

NaOH:*Ca(OH)*$_2$[c]	H_2O_2	*MALLS*[a]			*LS/Viscometry*[b]		
		$M_w \times 10^{-5}$	$M_n \times 10^{-5}$	R_{gz} (nm)	$M_w \times 10^{-5}$	$M_n \times 10^{-5}$	R_{gz} (nm)
1:0	no	3.40	2.13	36	3.29	1.88	41
1:0	yes	3.94	2.94	37	3.69	2.45	38
1:1	yes	3.03	2.15	31	2.81	1.74	39
0:1	yes	2.78	1.71	34	2.70	1.53	37
0:1[d]	no	3.64	2.20	34	3.50	1.94	38
1:0[e]	no	6.96	4.01	36	6.89	3.88	50

[a] Determined by multi-angle laser light scattering. [b] Determined by combination of light scattering at 90° and viscometry. [c] Ratio of NaOH to $Ca(OH)_2$ in milliequivalents. [d] First step in sequential extraction. [e] Second step in sequential extraction.

TABLE IV Molecular properties of hemicellulose B at peak maxima in fractions

NaOH:*Ca(OH)*$_2$[c]	*P*[d]	*MALLS*[a]		*LS/Viscometry*[b]		
		$M_w \times 10^{-5}$	R_{gz} (nm)	$M_w \times 10^{-5}$	R_{gz} (nm)	IV (dL/g)
1:0[e]	1	10.2(0.1)[f]	40(2)	12.4(0.1)	60(1)	3.7(0.1)
1:0	1	9.8(0.2)	38(2)	13.4(1)	56(2)	3.7(0.1)
1:1	1	8.5(0.7)	37(4)	10.4(0.6)	51(1)	3.6(0.1)
0:1	1	8.4(0.8)	39(2)	10.1(0.7)	51(1)	3.7(0.2)
0:1[e,g]	1	10.9(0.3)	37(1)	13.3(0.1)	53(2)	3.2(0.1)
1:0[e,h]	1	16.1(0.3)	37(1)	20.8(0.2)	58(1)	2.7(0.1)
1:0[e]	2	2.1(0.1)	31(3)	2.4(0.1)	25(1)	1.9(0.1)
1:0	2	2.4(0.1)	33(2)	2.8(0.1)	27(1)	1.1(0.1)
1:1	2	2.0(0.1)	28(4)	2.4(0.2)	26(1)	1.2(0.1)
0:1	2	1.8(0.2)	28(5)	2.3(0.1)	25(1)	1.9(0.1)
0:1[e,g]	2	3.0(0.1)	30(2)	3.0(0.1)	26(1)	1.7(0.1)
1:0[e,h]	2	3.3(0.1)	30(1)	3.4(0.1)	27(1)	1.6(0.1)

[a] Determined by multi-angle laser light scattering. [b] Determined by combination of light scattering at 90° and viscometry. [c] Ratio of NaOH to $Ca(OH)_2$ in milliequivalents. [d] Peak maxima as indicated by 90° light-scattering tracing in fractions 1 and 2. [e] No H_2O_2 treatment. [f] Standard deviation of triplicate analysis. [g] First step in sequential extraction. [h] Second step in sequential extraction.

Interestingly, uncorrected M_n values remained virtually unchanged after correction (uncorrected values not shown). Comparisons of corrected LS/Viscometry values with MALLS values reveal that M_n and M_w values from LS/Viscometry are lower, whereas R_{gz} values are higher. Molar mass values were in agreement within 10% or better by the two methods, whereas R_{gz} values differed as much as 38%. Nevertheless four of the six values agree within 15%. M_n and M_w for both methods of measurement follow the same trends with treatment.

Table IV contains molecular parameters at peak maximum for molecules in each distribution of the bimodal. Trends for the data shown in this table are comparable to those observed for the data in Table II.

CONCLUSIONS

We have demonstrated that hemicellulose B extracted from CF is comprised of a bimodal distribution of polysaccharides. The high-molar-mass distribution contains compact, probably highly branched polysaccharides, whereas the lower molar mass distribution contains less compact, probably less branched more linear polysaccharides. Although the distribution appears to be bimodel, one cannot rule out the possibility that within each of the macrodistributions there may be polysaccharide chains and that are very complex mixtures of different architectures.

There are a sufficient number of uncertainties in the use of both methods, so that it is difficult to say which method is best. For the particular case at hand, comparison reveals that both methods give reasonable agreement in global values for the measurement of moderately broad distributions of, polar macromolecules in an aqueous solution. Both methods indicate a bimodal distribution with fraction 1 containing an extremely compact structure. Only the LS/Viscometry method gives shape information on fraction 2, which indicates that molecules in fraction 2 are more extended than those in fraction 1 and perhaps less branched. The LS/Viscometry software and methodology, however, requires modification to handle a bimodal distribution case to obtain correct "global values".

References

[1] L.W. Doner and K.B. Hicks (1997). *Cereal Chem.*, **74**, 176.

[2] M.W. Rutenberg and W. Herbst (1957). U.S. Patent 2.801, 955.

[3] S.C. Fry (1988). In: *The Growing Plant Cell Wall: Chemical and Metabolic Analysis.* (John Wiley and Sons, New York).

[4] L.W. Doner, H.K. Chau, M.L. Fishman and K.B. Hicks (1998). *Cereal Chem.*, **75**, 408.

[5] M.L. Fishman, L. Rodriguez and H.K. Chau (1996). *J. Agric. Food Chem.*, **44**, 3182.

[6] L. Jeng and S.T. Balke (1993). *J. Appl. Polymr. Sci.*, **49**, 1375.

[7] M.L. Fishman, P. Cescutti, W.F. Fett, S.F. Osman, P.D. Hoagland and H.K. Chau (1997). *Carbohydr. Polymr.*, **32**, 213.

[8] TriSec GPC Software Manual, Version 2.7 (1994). (Viscotek Corp., Houston, TX), pp. A-17–A-18.

[9] P.J. Flory (1953). In: *Principles of Polymer Chemistry*. (Cornell University Press, Ithaca, NY), Chap. 14.

[10] P.J. Wyatt (1973). *Anal. Chim. Acta*, **272**, 1.

[11] L. Saulnier, C. Marot, E. Chanliaud and J.-F. Thibault (1995). *Carbohydr. Polymr.*, **26**, 279.

[12] R.L. Whistler and W.M. Corbett (1955). *J. Org. Chem.*, **21**, 694.

[13] R. Montgomery and F. Smith (1957). *J. Am. Chem. Soc.*, **79**, 695.

[14] M.L. Fishman, P. Cooke, B. White and W. Damert (1995). *Carbohydr. Polymr.*, **26**, 245.